Volume 1 | Number 1 | Jan 2013 | Pages 1–100

Analyst

www.rsc.org/analyst

ROYAL SOCIETY OF CHEMISTRY

ROYAL SOCIETY OF CHEMISTRY

www.rsc.org/analyst

ARTICLE TYPE

DNA methylation detection with end-to-end nanorod assembly-enhanced surface plasmon resonance

Xuemei Li, *[a] Ting Song, [b] and Xilin Guo [b]

The Au nanorod (AuNR) assembly-enhanced surface plasmon resonance（SPR）system coupling with polymerization and nicking reactions was developed for amplified detection of DNA methylation and adenine methylation (Dam) 10 methyltransferase (MTase) activity assay. The biosensor showed a good linear relationship between the SPR angle shift and the Dam MTase concentration over a range from 0.5 to 120 U/mL, with a detection limit of 0.2 U/mL. This study provided a sensitive platform to screen inhibitors for Dam 15 MTase and had a great potential to be further applied in early clinical diagnosis.

Surface plasmon resonance (SPR) sensors are powerful tools for label-free, real-time analysis of interfacial behaviors of various biological analytes and their interactions.[1] Their 20 unique abilities for characterizing and quantifying low molecular weight molecules is routinely used in a wide variety of research field, such as theranostics, clinic diagnosis, food safety and environmental monitoring.[2] With the growing availability of SPR instruments, it is also gaining popularity 25 for sensing applications and has been employed for the detection of cell,[3] protein,[4] and nucleic acid.[5] However, the use of the SPR method is impeded by the fact that the changes in the refractive index are often small, which has impeded further application of SPR in detection of trace targets in 30 complex biological samples. Different methods to enhance the sensitivities in SPR analyses have been explored,[6] including metal NPs,[7] graphene,[8] and dendrimer[9] as labels to enhance the refractive index change. The metallic NPs, especially gold nanoparticles (AuNPs), have been used as labels for SPR 35 amplification, which originated from the coupling between the localized surface plasmon of the NPs and the surface plasmon wave.[1a]

The sensitive and selective detection of biomarkers has great potentials in biological studies, since it is essentially

40

[a] School of Chemistry and Chemical Engineering, Linyi University, Linyi 276005, P. R. China
[b] Center of Cooperative Innovation for Chemical Imaging Functional 45 *Probes in Universities of Shandong, College of Chemistry, Shandong Normal University, Jinan 250014, P.R. China*
E-mail:xuemei_li@yeah.net; Fax: 86-539-8766867; Tel: 86-539-8766867.
† Electronic supplementary information (ESI) available: Experimental section and additional figures and discussions. See DOI:

50 important for early diagnosis of tumors. A number of amplification strategies have attracted considerable attention, because of their striking improvement for the detection sensitivity.[10] In our previous work, we demonstrated a series of amplification methods, such as strand-displacement 55 amplification (SDA), rolling-circle amplification (RCA), RNA ribozyme cyclic amplification, and the bio-bar-code technique.[11] Recently, we developed a SPR detection system based on a hybridization chain reaction (HCR) for amplified detection of DNA and small molecule.[12] In addition, there are 60 some reports on the combination of enzyme cyclic signal enhancement methods with SPR detection, in which AuNPs were used as SPR labels.[13] However, a SPR detection system combining nanoparticle assemblies with cyclic amplification strategy has not been reported yet.

65 DNA methylation is an important biological activity related to various pathogenic mechanisms of humans, such as some cardiovascular diseases and carcinomas.[14] Hence, detecting the DNA aberrant methylation level and the activity of methyltransferase (MTase) is imperative for rapid epigenetic 70 evaluation and early cancer diagnosis. In the present work, an Au nanorods (AuNRs) assembly-enhanced SPR system was developed for amplified detection of DNA methylation and adenine methylation (Dam) MTase activity assay. The palindromic duplex DNA probes were firstly methylated by DNA 75 Dam MTase and then cut by methylation-sensitive restriction endonuclease Dpn I. The released sequence worked as primer to induce polymerization and nicking reactions, producing a large amount of linker sequences. Subsequently, end-to-end (ETE) AuNR assemblies are linearly and periodically assembled to the 80 Au chip through the specific interactions between capture probes and linker sequences. The enhancement of the SPR signal was achieved by increasing the refractive index of the surface, due to the high molecular weight of AuNR assemblies.

The configuration and operation principle of the DNA 85 methylation detection and Dam MTase activity assay by AuNR assembly-enhanced SPR was depicted in Scheme 1. The double-stranded DNA (dsDNA) probe was formed by the self-hybridization of S_1 with a palindromic sequence of 5′-GATC-3′, which was specifically recognized by Dam MTase and Dpn I. In 90 the absence of Dam MTase, the reaction of DNA methylation has not been initiated, the dsDNA probes keeping intact. In the presence of Dam MTase, palindromic sequence of 5′-GATC-3′ was catalyzed to a methylated probe (5′-GAmTC-3′) by Dam

MTase with the help of S-adenosyl-L-methiolnine (SAM).[15] Then, this methylated dsDNA probe was cleaved into two parts by the methylation-sensitive restriction endonuclease Dpn I. The released part hybridized with the sequence S_2, which acted as template. In the presence of polymerase and the nucleotide mixture (dNTPs), the polymerase-induced reaction replicated the template and yielded the double-stranded domain that associates Nb.BbvCI nicking endonuclease, resulting in the nicking of the replicated single strand. The cleaved single strand generated a new site for the initiation of replication.[16] Thus, a large number of sequences **b** were produced.

The solution containing **b** was introduced into the gold chip, on which the thiolated capture DNA was anchored via sulfur-gold affinity. Subsequently, AuNR assemblies were linearly and periodically assembled to the Au chip through the specific interactions between S_4 and **b**. The enhancement of the SPR signal was achieved by increasing the refractive index of the surface, due to the high molecular weight of AuNR assemblies.
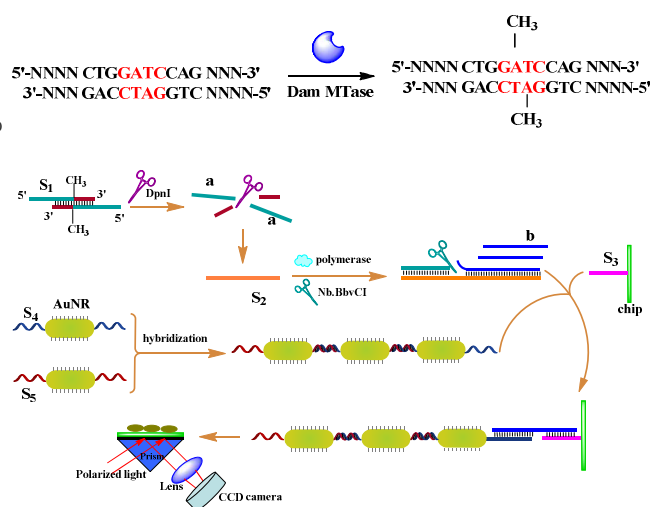

Scheme 1 Schematic illustration of DNA methylation detection based on ETE AuNR assembly-enhanced SPR.

Fig. 1 shows the TEM images of the AuNRs in different forms. The free AuNRs have lengths and diameters of 50 nm and 18 nm, respectively, with an aspect ratio of 2.8 (Fig. 1a). TEM observation confirmed that the Au nanorods have uniform and well-defined structure, and this feature was well maintained in the DNA modified hybrid (Figs. 1b,c). Preferential binding of thiol-terminated primers to the end facets of the NRs allowed for the ETE growth mode for the NR chains (Fig. 1d).

UV-vis spectra were employed to further characterize the assembly of the AuNRs. Gold nanorods are elongated nanoparticles whose extinction spectra exhibit two plasmon resonances, as shown in Fig. S1 in the EIS†. The transverse plasmon is the result of excitation across the nanorod diameter and is similar to plasmon resonances in spherical gold colloid. The longitudinal plasmon is due to excitation along the nanorod length. NR chains made from end-modified NRs can be approximated in terms of optical properties as nanowires (NWs).[17] The transverse plasmon for the ETE assembly changed

very little, whereas the longitudinal peak undergoes a red shift to 670 nm. Considering the geometry of the synthesized superstructure, one can consider their utilization as probes in surface-enhanced spectroscopies.
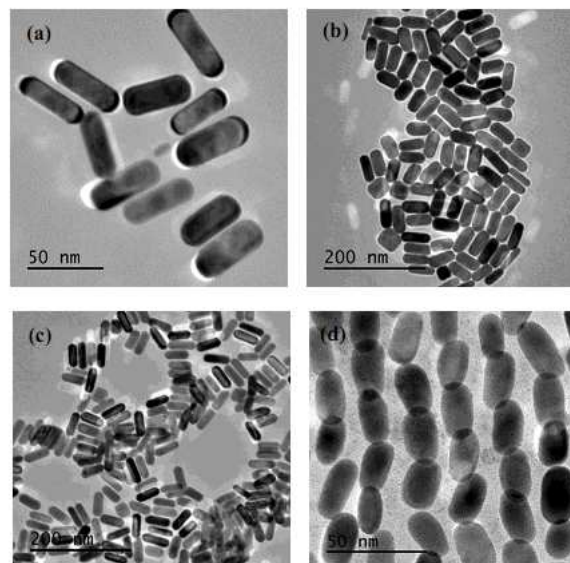
Fig. 1 TEM images of the free AuNRs (a), S_4-AuNRs (b), S_5-AuNRs (c), and ETE AuNR assemblies (d).

The fabrication process of the SPR aptasensor was characterized by electrochemical impedance spectroscopy (EIS), and the resulting voltammograms were displayed in Fig. 2. The bare gold electrode exhibited a very small semicircle domain with electron transfer resistance (Ret) of ~400 Ω. After immobilization of capture probe S_3 on the electrode, a big semicircle with Ret of ~1.5 kΩ was obtained. 6-Mercapto-1-hexanol (MCH) treatment induced a further increase in the electron transfer impedance. Addition of buffer solution and ETE probes produced no further impedance increase (Fig. 2A). Nevertheless, introduction of sequence **b** and ETE probes, a significantly large impedance was obtained (Fig. 2B), due to the introduction of ETE probes.
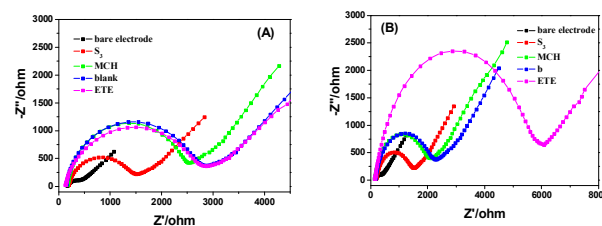
Fig. 2 Nyquist diagrams for the electrochemical impedance measurements of the gold electrode at different modification stages. (A) is for the addition of blank and (B) is for the addition of sequence **b**.

SPR was used to study the methylation process from the planar substrate, with injecting of the methylation reaction solution and the end-to-end AuNR assemblies into the fluidic channels separately, and a typical SPR response curve of this process was shown in Fig. S2 (EIS†). Compared with

the bare Au substrate, the modification of S_3 induced the increase of SPR angle due to the coverage of S_3 onto Au Chip. After S_3 functionalized substrate was incubated with produced **b** for 30 min, the SPR angle increased from 69.616 degree to 69.632 degree as a result of the hybridization process. Then the ETE AuNRs probes were introduced into the flow cell, and the SPR angle further increased 0.782 degree, corresponding to the loading of the ETE probes. In order to subtract background signal such as bulk refractive index change or environmental noise, two fluidic channels were used by serially flowing the ETE solution into a reference channel (no Dam MTase added) and the analytical channel. As shown in Fig. S2, small binding signal in curve **a** was expected, might due to the nonspecific adsorption of methylation production and the ETE probes. This background was substracted in the following experimental.

In order to carry out the experimental in short time, the methylation reaction solution and the ETE AuNR assemblies were mixed and injected at the same time, as described in the experimental section. To demonstrate the necessity for the coexistence of Dam MTase and Dpn I, SPR measurement of reaction was performed with the involvement of two enzymes. As shown in Fig. S3, in the absence of either Dam MTase or Dpn I, the palindromic dsDNA probe cannot be cleaved and no signal primer was produced even though it is in the presence of nicking enzyme. As a result, no sequence **b** was produced and no observable SPR signal was observed (blue and green lines). In contrast, in the presence of Dam MTase and Dpn I, the SPR angle increased with the reaction time in a sigmoidal fashion (red line).

To demonstrate the analytical performance of the proposed method, we measured the Dam MTase at various concentrations under the optimal conditions (see EIS† for optimazition). As shown in Fig. 3A, the SPR signal of the sensing system increased with increasing Dam MTase concentration. This is in accordance with the fact that under higher concentrations of Dam MTase, more sequences **a** are released, producing more **b**. The SPR signal was proportional to the Dam MTase concentration over from 0.5 to 120 U/mL. The regression equation is y=0.0049x+0.1527 with R^2=0.9875, in which x is the concentration of Dam MTase and y is the SPR angular shifts. A detection limit of 0.2 U/mL is estimated for Dam MTase from the slope and the standard deviation of the zero level (3× SDzero/slope), and is comparable to previously reported results with the lowest LOD of 0.1 U/mL.[18] The detection limit is 5 fold lower than that of with monomer AuNR as probe (see EIS†).
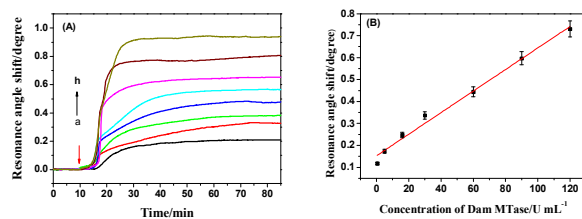
Fig. 3 (A) Real-time resonance angle responses of biosensor for Dam MTase detection with ETE AuNR assembly probes. The concentration of

Dam MTase from a to h: 0, 0.5, 5.0, 15, 30, 60, 90, 120 U/mL. (B) Calibration curve of the determination of Dam MTase with ETE AuNR assembly probes.

In order to evaluate the specificity of this assay, the SPR response of the sensing system to other DNA MTase such as AluI MTase, CpG MTase and GpC MTase were also investigated. All results were displayed in Fig. 4. It was found that 60 U/mL Dam MTase could induce a significant SPR increase, whereas all other DNA MTase at the same concentration did not induce an obvious SPR enhancement (the signal for other DNA MTase was 16-23% of Dam MTase), demonstrating that our sensing system has a high specificity for Dam MTase.
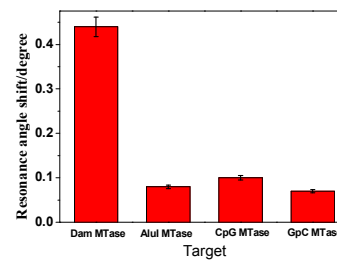
Fig. 4 Selectivity of the proposed method. The concentration of all DNA MTase is 60 U/mL. Error bars show the standard deviation of three experiments.

To investigate the applicability of the method in real biological environment, the detection of Dam MTase in cytosol was performed. The HeLa cell cytosol spiked with different concentrations of Dam MTase were detected with our method. As presented in Table S2, a series of five parallel measurements of samples yielded relative standard deviation less than 8.2%, recoveries were obtained with 93.4-112%. These results indicated that the proposed assay showed good applicability in practical condition.

Dam MTase has become a promising target for antimicrobial drug development, since that Dam MTase inhibitors have broad antimicrobial action.[19] For testing the potential of the proposed system to evaluate and screen the inhibitor of Dam MTase, four kinds of antibiotics and two kinds of anticancer drugs as model inhibitors had been chosen as models.[18a] As shown in Fig. S7 (EIS†), the benzylpenicillin sodium, gentamycin sulfate, and fluorouracil could distinctly inhibit the methylation. The inhibition by 5-fluorouracil was the most serious one, which may decrease the activity of Dam MTase by about 46%. Nonetheless, the rest of the antibiotics and anticancer drugs had hardly effect on the methylation.

In conclusion, we have demonstrated an SPR platform for sensitive DNA methylation detection and Dam MTase activity assay based on cycle amplification strategy of polymerization and nicking reactions and of SPR signal amplification with ETE AuNR assemblies. The Nb.BbvCI nicking endonuclease assisted cleavage process can produce a large number of cleaved **b** fragments with the initiation of a few methylation products, which then act as linker to introduce the AuNR assemblies onto the Au chip. Furthermore, the AuNR assemblies functioned as a signal-enhancing scaffold, inducing significant enhancement of the SPR signals. The

biosensor showed a good linear relationship between the SPR angle shift and the Dam MTase concentration and the LOD can achieve to 0.2 U/mL level, had a great potential to be further applied in early clinical diagnosis.

Notes and references

1   (*a*) S. Zeng, D. Baillargeat, H.-P. Hod and K.-T. Yong, *Chem. Soc. Rev.*, 2014, **43**, 3426–3452; (*b*) J. Homola, *Chem. Rev.*, 2008, **108**, 462–493.

2   C. Situ, J. Buijs, M. H. Mooney and C. T. Elliott, *Trends Anal. Chem.*, 2010, **29**, 1305–1315.

3   (*a*) P. N. Abadian, C. P. Kelley and E. D. Goluch, *Anal. Chem.* 2014, **86**, 2799−2812; (*b*) Y. Yanase,T. Hiragun, T. Yanase, T. Kawaguchi, K. Ishii and M. Hide, *Biosens. Bioelectron.*, 2012, **32**, 62−68.

4   (*a*) X. Yi, Y. Hao, N. Xia, J. Wang, M. Quintero, D. Li and F. Zhou, *Anal. Chem.*, 2013, **85**, 3660–3666; (*b*) S. Krishnan, V. Mani, D. Wasalathanthri, C. V. Kumar and J. F. Rusling, *Angew. Chem., Int. Ed.,* 2011, **50**, 1175–1178.

5   (*a*) Z. Zhang, Q. Cheng and P. Feng, *Angew. Chem., Int. Ed.*, 2009, **48**, 118–122; (b) L. G. Carrascosa, A. A. I. Sina, R. Palanisamy, B. Sepulveda, M. A. Otte, S. Rauf, M. J. A. Shiddiky and Matt Trau, *Chem. Commun.*, 2014, **50**, 3585–3588.

6   (*a*) G. Pelossof, R. Tel-Vered, X.-Q. Liu and I. Willner, *Chem. – Eur. J.*, 2012, **17**, 8904–8912; (*b*) B. T. Houseman, J. H. Huh, S. J. Kron and M. Mrksich, *Nat. Biotechnol.*, 2002, **20**, 270–274.

7   H. R. Jang, A. W. Wark, S. H. Baek, B. H. Chung and H. J. Lee, *Anal. Chem.*, 2014, **86**, 814−819.

8   W. Hu, G. He, H. Zhang, X. Wu, J. Li, Z. Zhao, Y. Qiao, Z. Lu, Y. Liu and C. M. Li, *Anal. Chem.*, 2014, **86**, 4488–4493.

9   S. K. Choi, A. Myc, J. E. Silpe, M. Sumit, P. T. Wong, K. McCarthy, A. M. Desai, T. P. Thomas, A.Kotlyar, M. M. B. Holl, B.G. Orr and J. R. Baker, *ACS Nano*., 2013, **7**, 214–228.

10 H. Q. Zhang, F. Li, B. Dever, X. F. Li and X. C. Le, *Chem. Rev.,* 2013, **113**, 2812–2841.

11 (*a*) X. Li, J. Liu and S. Zhang, *Chem. Commun.*, 2010, **46**, 595–597; (*b*) S. Zhang, J. Xia and X. Li, *Anal. Chem.*, 2008, **80**, 8382–8388; (*c*) X. Li, L. Wang, C. Li, *Chem.-Euro. J.*, 2015, **21**, 6817-6822; (*d*) X. Li, T. Ding, L. Sun and C. Mao, *Biosens. Bioelectron*., 2011, **30,** 241–248; (*e*) R. Ren, L. Wang, T. Ding and X. Li, *Biosens. Bioelectron.*, 2014, **54**, 122–127.

12 X. Li, Y. Wang, L. Wang and Q. Wei, *Chem. Commun.*, 2014, **50,** 5049–5052.

13 (*a*) P. He, L. Liu, W. Qiao and S. Zhang, *Chem. Commun.*, 2014, **50**, 1481–1484; (*b*) P. He, W. Qiao, L. Liu and S. Zhang, *Chem. Commun.*, 2014, 50, 10718–10721; (*c*) G. Yao, R. Liang, X. Yu, C. Huang, L. Zhang and J. Qiu, *Anal. Chem.*, 2015, **87**, 929–936.

14 (a) B. E. Bernstein, A. Meissner and E. S. Lander, *Cell,* 2007, **128**, 669−681; (b) C. Frauer, H. Proc. Leonhardt, *Natl. Acad. Sci. U.S.A.*, 2011, **108**, 8919−8920.

15 Y. Zeng, J. Hu, Y. Long and C. Zhang, *Anal. Chem.*, 2013, **85**, 6143−6150.

16 A. R. Connolly and M. Trau, *Angew. Chem. Int. Ed.,* 2010, **49**, 2720–2723.

17 W. Wei, S. Li, L. D. Qin, C. Xue, J. E. Millstone, X. Y. Xu, G. C. Schatz and C. A. Mirkin, *Nano Lett.,* 2008, **8**, 3446–3449.

18 (*a*) X. Wei, X. Ma, J. Sun, Z. Lin, L. Guo, B. Qiu and G. Chen, *Anal. Chem.*, 2014, **86**, 3563–3567; (*b*) X. Ouyang, J. Liu, J. Li and R. Yang, *Chem. Commun.*, 2012, **48**, 88–90; (*c*) X. Zhao, L. Gong, X. Zhang, B. Yang, T. Fu, R. Hu, W. Tan and R. Yu, *Anal. Chem.*, 2013, **85**, 3614−3620.

19 D. M. Heithoff, R. L. Sinsheimer, D. A. Low and M. J. Mahan, *Science,*1999, **284**, 967−970.

Analyst Accepted Manuscript